Photonic-Assisted Analog-to-Digital Conversion Based on a Dispersion-Diversity Multicore Fiber

Sergi García, Mario Ureña, and Ivana Gasulla, *Senior Member, IEEE*

(Invited Paper)

***Abstract*—Multigigabit-per-second photonic-assisted time-interleaved analog-to-digital conversion (ADC) built upon a dispersion-diversity multicore fiber (MCF) is proposed and experimentally demonstrated for the first time to our knowledge. Tunable true-time delay line operation for the analog signal replicas is provided by the different cores of a heterogeneous MCF, which feature different radial dimensions and GeO_2 dopant concentrations. Continuous real-time ADC tunability with the optical wavelength is experimentally demonstrated by time interleaving 5 digitized channels achieving equivalent sampling rates of 25, 50 and 125 GS/s for optical wavelengths of 1538, 1534 and 1531.6 nm, respectively. These values are beyond the 10.25-GS/s sampling rates offered by commercial electronic ADCs. One of the advantages of using a MCF for the parallel channels relies on the fact that all the cavities are subject to similar environmental conditions. The introduction of space and dispersion diversities provided by MCFs in photonic-assisted ADCs brings benefits in terms of size, weight, and power consumption reduction along with system flexibility and stability improvement. This is of particular relevance in those application scenarios where an optical fiber link is required to distribute the signal, such as fiber distributed sensing networks, as well as access networks for radar systems or next-generation wireless communications.**

***Index Terms*—Analog-to-digital converters, chromatic dispersion, multicore fibers, space-division multiplexing, time-interleaving.**

I. Introduction

THE exploitation of photonic technologies to enable analog-to-digital conversion (ADC) has proven essential to overcome the bottleneck of their electronic counterparts, mainly in terms of bandwidth and timing jitter, [1], [2], [3]. This benefit is of particular interest in next-generation information paradigms such as high-capacity optical networks, radar and electronic warfare, remote sensing, imaging, as well as advanced test instrumentation, which demand ADCs with ever-increasing sampling rates and bandwidth along with adequate accuracy, [4], [5], [6], [7], [8].

Over the past few decades, a rich variety of photonics techniques for wideband ADCs have been developed. Starting from optically clocked configurations applying time interleaving of a set of optical samples [9], [10]; wavelength division sampling where the signal is modulated over chirped broadband pulses and wavelength demultiplexed [11]; to photonic time stretching schemes where the electrical signal is compressed by stretching the waveform in time before being digitized for instance, by propagating the signal through a dispersive fiber medium, [12]. Furthermore, high-speed photonic sampling ADC using both time and wavelength interleaving in an ultra-short optical pulse train has been demonstrated recently, [13], but this approach requires the use of multiple lasers besides the WDM multiplexing devices. Data recovery via fully convolutional neural networks has also been applied to photonic ADC lately [3].

Among the different classes in which photonic ADCs can be divided, photonic-assisted ADCs, where electronics benefit from the inherent advantages of photonics to enhance some of its limiting properties while the sampling and quantization processes are made by electronic ADCs, [1], are particularly interesting due to their direct compatibility with current optical communications networks bringing, as a consequence, a cost-effective solution. Up to date, the sampling rate of commercial electronic ADCs is limited to 10.25 GS/s, [14]. The main idea behind photonic-assisted ADC architectures relies on the incorporation of a set of N parallel electronic ADCs to process, at the same time, N different replicas of the incoming signal to increase the effective sampling rate of the overall ADC beyond the limits of a single electronic ADC while allowing real-time operation.

We have previously proposed the exploitation of dispersion-diversity multicore fibers (MCF) [15] to provide parallel optical and microwave signal processing while the signal is being distributed with increased compactness and reduced power consumption, along with improved performance versatility and flexibility [16], [17], [18], [19], [20], [21], [22]. The so-called dispersion-diversity MCF involves tailoring "à la carte" the chromatic dispersion of each individual fiber core. Combining this property with the space and optical wavelength degrees of freedom in a single fiber link opens the way to a

Manuscript received 23 February 2023; revised 7 April 2023; accepted 10 April 2023. Date of publication 17 April 2023; date of current version 28 April 2023. This work was supported in part by ERC Consolidator under Grant 724663, in part by the Spanish Ministerio de Ciencia e Innovación under Grant PID2020-118310RB-100, in part by the Generalitat Valenciana Advanced Instrumentation for World Class Microwave Photonics Research under Grant IDIFEDER/2018/031, in part by Generalitat Valenciana PROMETEO/2021/15 Research Excellency Award, and in part by the Universitat Politècnica de València PAID-10-21 fellowship for Sergi García. *(Corresponding author: Sergi García.)*

The authors are with the Institute of Telecommunications and Multimedia Applications, Universitat Politècnica de València, 46022 Valencia, Spain (e-mail: sergarc3@iteam.upv.es; maurgis@iteam.upv.es; ivgames@iteam.upv.es).

Color versions of one or more figures in this article are available at https://doi.org/10.1109/JSTQE.2023.3267507.

Digital Object Identifier 10.1109/JSTQE.2023.3267507

This work is licensed under a Creative Commons Attribution-NonCommercial-NoDerivatives 4.0 License. For more information, see https://creativecommons.org/licenses/by-nc-nd/4.0/

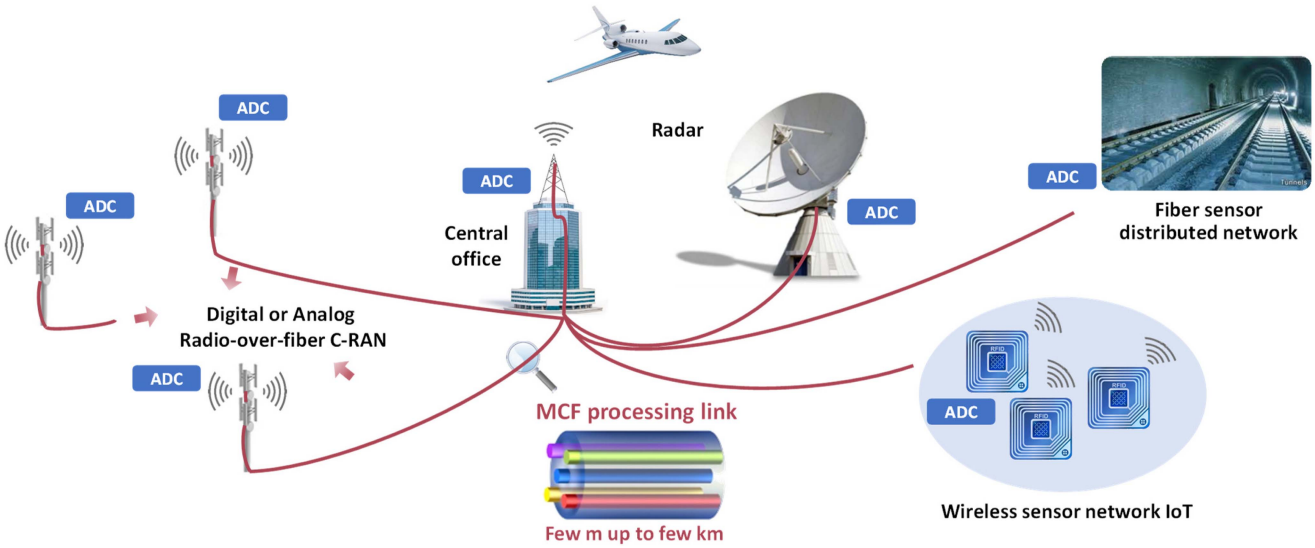

Fig. 1. Representative application scenarios for photonic-assisted analog-to-digital conversion based on a dispersion-diversity multicore fiber link, including fiber distributed sensing networks, as well as access networks for radar systems or next-generation wireless communications.

comprehensive range of dispersion-managed digital and analogue signal processing applications. Representative application scenarios include interference-controlled signal distribution in Multiple-Input Multiple-Output configurations, parallel chromatic dispersion compensation, time differentiation and integration, Fourier transformation, self-imaging phenomena (Talbot effects) to provide pulse repetition rate multiplication, waveform generation and shaping, optical beamforming for phased-array antennas, radiofrequency signal filters, instantaneous radiofrequency measurement and multicavity optoelectronic oscillation, among others [17].

Parallel signal management in most of the above-mentioned areas involves recombination of a given set of signal replicas with different time group delays, what can be provided in a continuously tunable way by the dispersion-diversity MCF. We propose in this work to apply the same principle to enable multigigabit-per-second photonic-assisted time-interleaved ADC, where the sampling rate can be increased by a factor given by the number of fiber cores *N*. The rationale behind this approach lies in the application of our tunable MCF-based true-time delay line (TTDL) to provide and control the required multiple time-delay replicas of the analog signal. After synchronous low-rate sampling by electronic commercial ADCs, the replicas are properly recombined to recover the final high-rate digitized signal.

Beyond the benefits brought by photonic-assisted time-interleaving technologies to enable high-bandwidth ADCs, our dispersion-diversity multicore-fiber architecture allows for real-time sampling rate tunability and remote system reconfigurability, providing higher degrees of compactness, flexibility and versatility. We must note, in first place, that a single optical fiber provides the set of time delays required by exploiting the space degree of freedom, i.e., without needing WDM configurations that will increase cost and power consumption. All in all, if needed, one can exploit not only the space but also the optical wavelength degree of freedom, by injecting an array of *M* optical wavelengths into each core. This will lead to *N* x *M* samples and, therefore, a parallel set of simultaneous time-interleaved ADCs (each one working with a different sampling rate, which is tunable). Second, the use of the optical fiber link not only to transmit the data signal, but also to perform analog-to-digital conversion "on the fly", enables remote system reconfigurability. As illustrated in Fig. 1 for a representative application scenario, the ability to process the signal while it is being distributed gains importance where the existence of the fiber link (from several hundreds of meters up to a few km) is mandatory. We are referring, for instance, to radio access networks for 5G and Beyond wireless communications or radar systems, as well as distributed fiber sensing networks.

In this paper, we propose and experimentally demonstrate, for the first time, photonic analog-to-digital conversion based on a dispersion-diversity MCF. First, we develop the principle of operation based on the tunable MCF-based TTDL and the application of time interleaving. Then, we describe the main characteristics of the fabricated ad hoc heterogeneous MCF link. Continuous real-time ADC tunability with the optical wavelength is experimentally demonstrated by time interleaving 5 signal replicas achieving equivalent sampling rates up to 125 GS/s. Finally, we provide further discussion about the performance limits of the proposed architecture.

II. Time-Interleaved Dispersion-Diversity-MCF Concept

Fig. 2 represents the operation principle of the proposed time-interleaved photonic-assisted ADC architecture. As every time-interleaved ADC system, the fundamental idea consists of sampling a given input analog signal by means of a set of *N* parallel digitizers of lower sampling rate, and the subsequent application of digital interleaving as to increase the overall system sampling rate by a factor of *N*. In our approach, the key building block is a *N*-core dispersion-engineered heterogeneous

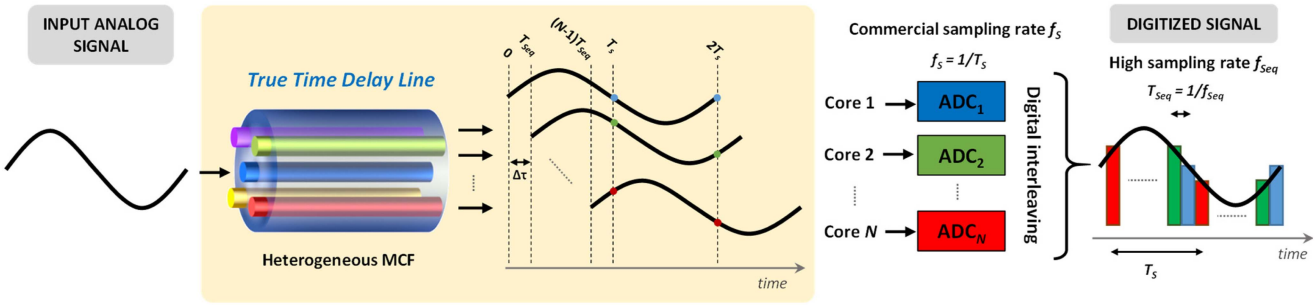

Fig. 2. Operation principle for the proposed photonic-assisted time-interleaved ADC architecture based on a dispersion-diversity heterogeneous MCF.

MCF that has been designed to behave as a tunable sampled TTDL. As Fig. 2 shows, the input analog signal is split and injected into the N cores of the MCF to obtain, at the fiber output, N time-delayed replicas of the input signal. The replicas are then sampled by a set of N parallel electronic ADCs sequentially clocked at a sampling rate f_s. Finally, they are recombined to properly perform the digital interleaving that leads to a digitized signal with an equivalent sampling rate $f_{s,eq} = N{\cdot}f_s$.

The differential group delay (DGD) between adjacent replicas $\Delta\tau$, is synthetized by the MCF itself. The MCF is dispersion-engineered to provide a common $\Delta\tau$ between each pair of adjacent cores, which can also be tuned with the optical wavelength as

$$\Delta\tau\,(\lambda) = \Delta D \cdot (\lambda - \lambda_0) \tag{1}$$

being λ_0 the anchor wavelength where all the cores experience an identical group delay, $\tau_n(\lambda_0) = \tau_0, n = 1, 2, \ldots, N$, and $\Delta D = D_n - D_{n\text{-}1}, n = 2, 3, \ldots, N$, the incremental chromatic dispersion between adjacent cores at λ_0, [16], [17].

For the photonic-assisted time-interleaved ADC to increase the sampling rate of the parallel electronic ADCs, f_s, by a factor N, the DGD between cores must satisfy the relation

$$T_s = 1/f_s = N \cdot \Delta\tau \tag{2}$$

being T_s the sampling time of the electronic ADCs. Then, the equivalent sampling rate for the photonic-assisted time-interleaved ADC results

$$f_{s,eq} = N \cdot f_s = 1/\Delta\tau \tag{3}$$

that is, the equivalent sampling time equals the DGD between cores, $T_{s,eq} = \Delta\tau$. Since $\Delta\tau$ can be tuned with the operation wavelength of the optical source, we see from (3) that the equivalent sampling rate can be tuned adaptively depending on the operation optical wavelength. Although the electronic ADCs have fixed sampling rate, parallel configurations can be implemented, simultaneously while the signals are being distributed through a single dispersion-engineered heterogeneous MCF link. For instance, having a matrix of MxN electronic ADCs with sampling rates $f_{s,m}$ would allow the implementation of M parallel time-interleaved ADCs operating at different optical wavelengths with the condition that the ADCs' sampling time $T_{s,m}$ of each row m satisfies (2).

From Fig. 2, we can easily follow that the proposed architecture supports real time operation. Given an input real-time analog signal, we see that either the optical replication or the parallel sampling is performed in continuous time. For the digital interleaving step, an inverse DGD stage can be applied to undo the different DGD applied to each replica and thus recover the sampling of the original signal for the digitized signal, which is compatible with continuous time operation.

TABLE I
CORE REFRACTIVE INDEX DESIGN PARAMETERS. DESIGNED AND MEASURED CHROMATIC DISPERSIONS AT $\lambda_0 = 1530$ NM

Core n	*Designed*					*Measured*
	a_1 (μm)	Δ_1 (%)	a_2/a_1	w/a_1	D (ps/km/nm)	D_{CSE} (ps/km/nm)
1	3.3	0.335	1.758	0.970	14.30	13.85
2	3.2	0.300	0.750	1.281	15.30	14.95
3	3.5	0.315	1.286	1.143	16.30	16.35
4	3.7	0.301	1.000	0.973	17.30	17.30
5	4.8	0.293	1.208	0.625	18.30	18.25
6	5.0	0.287	0.920	1.200	19.30	19.30
7	5.3	0.279	0.623	1.132	20.30	20.30

III. DISPERSION-DIVERSITY MULTICORE FIBER

We have developed a dispersion-diversity heterogeneous MCF for tunable TTDL operation. It comprises seven distinct trench-assisted cores drawn from seven different preforms and placed in a hexagonal disposition. The refractive index profile of each core was tailored independently to satisfy a common group delay at the anchor wavelength $\lambda_0 = 1530$ nm with linearly incremental chromatic dispersion values, D_n, ranging from 14.3 to 20.3 ps/km/nm, respectively for cores 1 up to 7, with an incremental chromatic dispersion $\Delta D = 1$ ps/km/nm, [17]. Table I gathers the design parameters of each core refractive index profile along with the measured chromatic dispersions. Each core has different radial dimensions and GeO_2 dopant concentrations. The core radii a_1 range from 3.2 up to 5.3 μm, with core-to-cladding relative index differences, Δ_1, ranging from 0.279% up to 3.335%. Each core layer is followed by a pure silica inner cladding of variable width a_2 and a 1%-F-doped trench layer of variable width w. The core arrangement inside the cladding was set to minimize intercore crosstalk by ensuring adjacent cores have the maximum effective refractive index

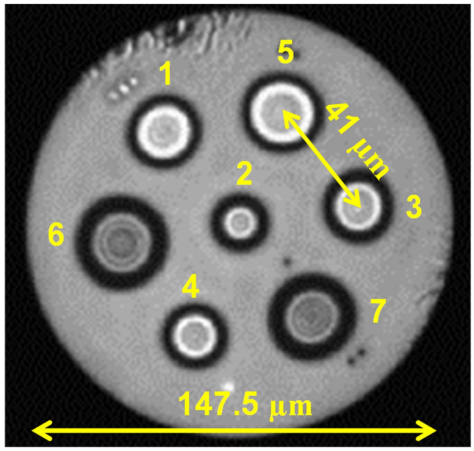

Fig. 3. Photograph of the cross-section area of the fabricated heterogeneous MCF.

difference. From that, we find the critical bending radius for this fiber is 8.55 cm.

Fig. 3 shows a photograph of the cross-section of the fabricated MCF, where we appreciate the different radial dimensions of each core. A total length of 5.038 km was drawn by the company YOFC. The cladding diameter is 147.5 μm and the average core pitch is 41 μm. Accounting for both the fiber link and the fan-in/fan-out devices, the measured total insertion losses range from 4.6 to 7.7 dB, while the measured inter-core crosstalk is below -26.9 dB at 1560 nm in the worst-case (cores 1 and 2). A complete experimental characterization of this MCF, including among others crosstalk time variation and spectra, influence of temperature on the fiber skew, and spectral chromatic dispersion behavior, can be found in [17].

Table I compares the designed and the measured chromatic dispersion for each core. We measured the chromatic dispersion by evaluating the carrier suppression effect on the radiofrequency response of the 5-km fiber link. We observe a good agreement between design and fabrication for cores 3 to 7, which deliver a differential chromatic dispersion ΔD of 1 ps/km/nm. In contrast, cores 1 and 2 present a deviation in the chromatic dispersion. This is likely caused by fabrication inaccuracies as small cores are more sensitive to radial variations.

Next, we evaluated the capability of this fiber to provide continuous tunable TTDL operation. We measured the DGD at different optical wavelengths from 1530 to 1560 nm using an optical interferometric technique [23]. Figure 4(a) depicts the measured DGDs as a function of the optical wavelength with respect to core 7. Circle markers represent the measured values and solid lines the trend with the optical wavelength. In line with the measured dispersion values, we appreciate that cores 3 to 7 present a linearly incremental delay with the optical wavelength without significant deviation and non-linearities within a 30-nm range. Figure 4(b) illustrates the measured spectral space-diversity differential group delay $\Delta\tau$ for cores 3 to 7, where red-filled squares represent the mean measured differential group delays, error bars show their maximum deviation, and the black solid line represents the trend line for the mean values.

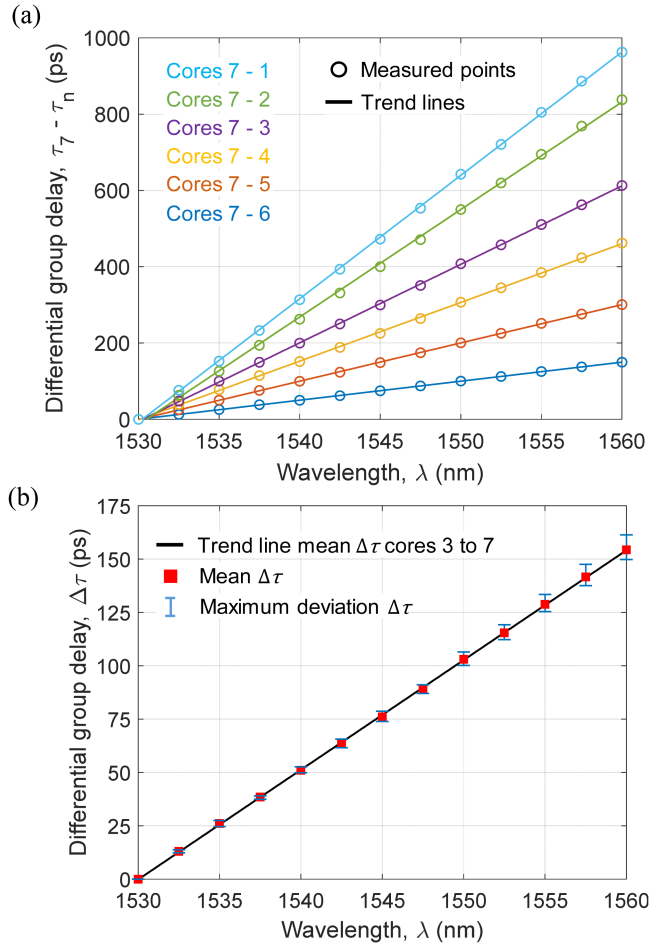

Fig. 4. (a) Measured spectral DGD with respect to core 7 ($\tau_7 - \tau_n$), and b) mean value of the measured DGD between adjacent cores ($\Delta\tau$) for cores 3 to 7 (red-filled squares), along with the maximum deviation (error bars) and the trend line for the mean $\Delta\tau$ (black line).

Therefore, in the space-diversity domain (i.e., signal samples are provided by different cores for a given input optical wavelength), we achieved up to 5-sample tunable TTDL operation with a tunable differential delay from 0 up to 150 ps when the optical wavelength is varied from 1530 to 1560 nm. Even so, in the wavelength-diversity domain (i.e., signal samples are provided by different input optical wavelengths within a given core), we must note that all cores can be employed as independent tunable TTDLs. In addition, cores 1 and 2 could be exploited to transmit independent data channels, or included as part of the space-diversity TTDL for other applications in which constant time delays are not necessary, [24].

IV. Photonic Analog-to-Digital Conversion Experimental Results

The unique properties of the fabricated dispersion-diversity MCF grant the implementation of distributed high-speed ADC by using the proposed optical time-interleaving technique. One of the main advantages of this approach relies on the continuous time delay tunability of the implemented TTDL, which allows adaptive sampling rates by simply tuning the optical wavelength,

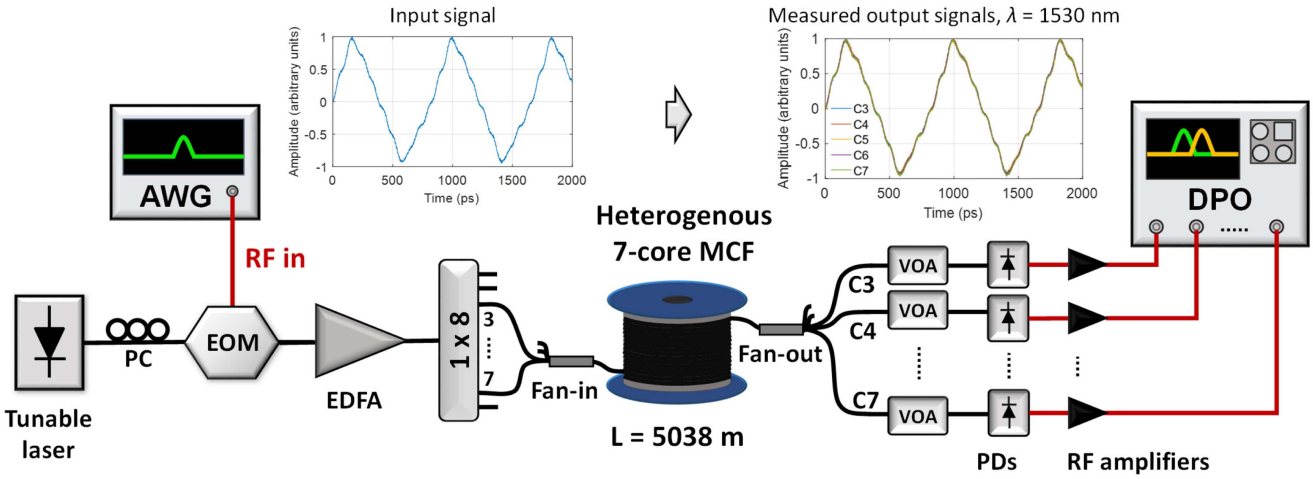

Fig. 5. Schematic representation of the experimental setup for the proposed photonic-assisted time-interleaved ADC based on a dispersion-diversity heterogeneous MCF. Upper graphs represent the measured RF input signal (left) and the measured received signals from cores 3 up to 7 in the DPO when the laser operates at the optical wavelength of 1530 nm. PC: polarization controller; AWG: Arbitrary waveform generator; EOM: electro-optic modulator; EDFA: Erbium doped fiber amplifier; MCF: Multicore fiber; VOA: Variable optical attenuator; PD: Photodetector; RF: radiofrequency; DPO: Digital phosphor oscilloscope.

adding a new degree of system flexibility. Fig. 5 depicts the experimental setup for the proposed photonic-assisted time-interleaved ADC. As the driving RF signal, we use a periodic triangular waveform with a period of 800 ps generated by an arbitrary waveform generator. The RF signal is modulated onto the optical carrier coming from a tunable laser via an intensity modulator. The modulated signal is then amplified and injected into cores 3 to 7 of the heterogeneous MCF, which, depending on the operation optical wavelength of the tunable laser, apply a particular differential group delay to the propagated signals. At the optical wavelength $\lambda = 1530$ nm (anchor wavelength), the time delay experienced in each of the MCF cores is identical, in accordance with Fig. 4. As the operation wavelength of the optical source increases, the differential time delay between signal samples increases linearly with the optical wavelength. This property is accomplished thanks to the chromatic dispersion diversity provided by the fabricated MCF. At the fiber output, the amplitude of each signal is adjusted by means of a variable optical attenuator (VOA). The samples are then photodetected and amplified independently and visualized in a digital phosphor oscilloscope (DPO). The measured waveforms are digitally sampled and time-interleaved to obtain the equivalent sampling rate of the photonic-assisted ADC. Note that, due to the lack of capability to physically implement the whole ADC process in our laboratory, both the sampling and time-interleaving procedures are made by computer means. For each optical wavelength, the captured waveforms are digitally sampled at the corresponding f_s and the resulting sampled waveforms are adequately time interleaved by applying the reverse differential group delay.

Fig. 6 illustrates the implemented ADC process for different optical wavelengths. Figures 6(a)–(c) show the measured waveforms in the DPO for each MCF core at $\lambda = 1531.6$, 1534 and 1538 nm, respectively. We see how the differential time delay between samples increases as the optical wavelength breaks away from the anchor wavelength of 1530 nm. In particular, the differential time delay between adjacent samples results in $\Delta\tau = 8$, 20 and 40 ps, respectively for $\lambda = 1531.6$, 1534 and 1538 nm, as expected from Fig. 4(b). According to (2), the required sampling rates for the parallel electronic ADCs are 25, 10 and 5 GS/s, respectively for $\lambda = 1531.6$, 1534 and 1538 nm. Figures 6(d)–(f) represent the temporal digital sampling applied to each waveform at the previous sampling rates. Here, the signal sampling is performed digitally to emulate the sampling made by electronic ADCs operating at the corresponding sampling rates. After the electronic ADCs, the different signals are time-interleaved to obtain the equivalent sampling rate for the photonic-assisted ADC, $f_{s,eq} = 5{\cdot}f_s$. Figures 6(g)–(i) show the time-interleaving process, where the equivalent sampling rate of the photonic-assisted ADC, $f_{s,eq}$, is increased up to 125, 50 and 25 GS/s, respectively for $\lambda = 1531.6$, 1534 and 1538 nm. All in all, the proposed photonic-assisted time-interleaved ADC reaches a sampling rate N times higher than that of the electronic ADCs used, being N the number of samples of the TTDL. In our experiment, $N = 5$, so that we require 5 electronic ADCs with lower sampling rate to achieve a high-speed ADC by performing the optical replication and time-interleaving processes.

Fig. 7 illustrates the relation between the required sampling rate for the electronic ADCs (orange) and the equivalent sampling rate obtained with the proposed MCF-based ADC (blue) as a function of the operation wavelength. As a limit case, at the optical wavelength of $\lambda = 1534$ nm, the differential time delay between samples is $T_s = 20$ ps, so that, by (2), the required sampling rate for the electronic ADCs is 10 GS/s, which is the current sampling rate limit for commercial electronic ADCs. At this operation wavelength, however, the equivalent sampling rate for the proposed MCF-based photonic-assisted ADC reaches 50 GS/s.

V. Discussion

The major limitations that can affect time-interleaved ADCs are related to synchronization mismatches between the parallel channels, which could lead to severe penalties on the

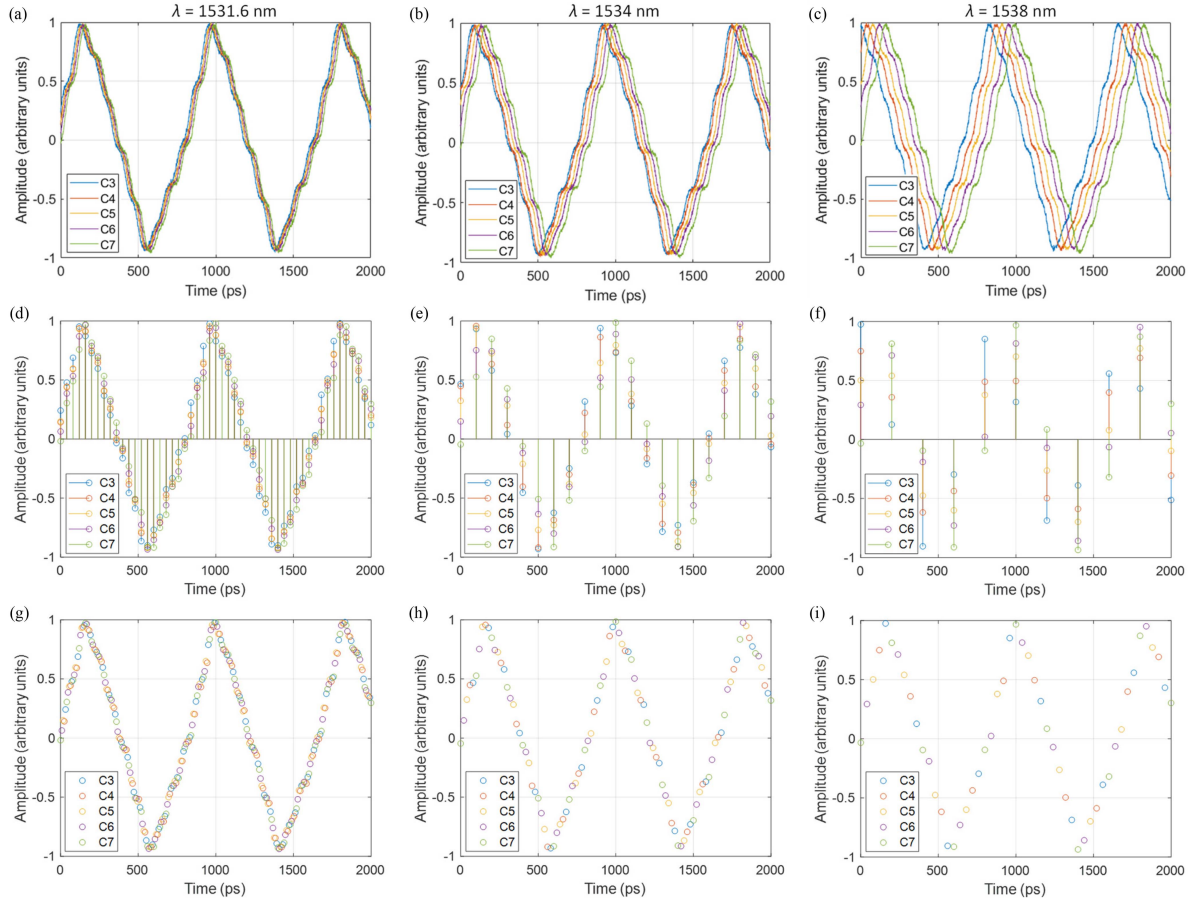

Fig. 6. Measured experimental results for the proposed photonic-assisted time-interleaved ADC based on a dispersion-diversity heterogeneous MCF at the optical wavelengths of (a), (d), (g) 1531.6 nm, (b), (e), (h) 1534 nm, and (c), (f), (i) 1538 nm. (a-c) Measured waveforms for cores 3 up to 7; (d-f) sampled waveforms at sampling rates $f_s = 25$, 10 and 5 GS/s, respectively; (g-i) resulting time-interleaved signals where the overall ADC sampling rate is increased up to $f_{s,eq} = 125$, 50 and 25 GS/s, respectively.

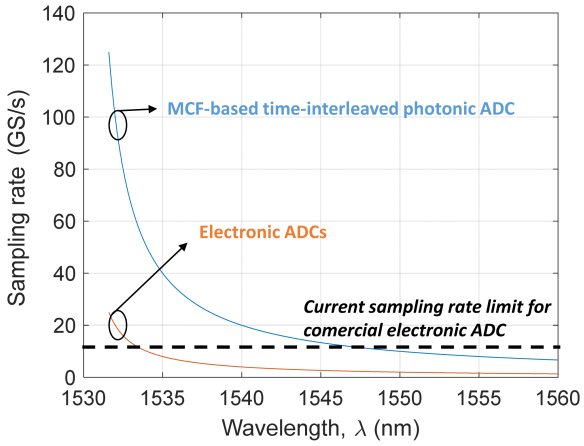

Fig. 7. Comparison between the sampling rate required for the parallel electronic ADCs (orange) and the resulting sampling rate for the MCF-based time-interleaved photonic ADC (blue) as a function of the optical wavelength.

signal-to-noise and distortion ratios and cause a considerable reduction on the ADC effective number of bits (ENOB), [12], [25], [26]. In first place, the signal amplitudes require proper management to guarantee maximum similarity between the replicas carried out by the parallel channels to minimize undesirable effects caused by these imbalances. In this regard, amplitude equalization through a set of VOAs is indispensable at the input of the electronic ADCs, as shown if Fig. 6.

In second place, sampling timing errors can highly degrade the ADC performance and become the dominant factor that limits the applicability of this approach. We can distinguish between 2 types of timing errors attending to its nature: random and deterministic. Random jitter is caused by noise and/or environmental effects during fiber propagation. Deterministic timing errors relate to time delay deviations from the theoretical $\Delta\tau$ (which is different in each pair of adjacent cores), and therefore will not change with time. These time delay deviations are caused by the mismatch between the actual and ideal chromatic dispersion values, consequence of fiber fabrication inaccuracies.

Random jitter is one of the main parameters that determine the performance of an ADC. Up to date, commercial ADCs can reach jitter values as low as 50 fs, with typical values ranging from 60 to 80 fs. The use of parallel channels, however, can cause clock synchronization skews that can increase the time uncertainty and thus degrade the jitter performance of the resulting ADC. Thus, as in every time-interleaved ADC, precise clock synchronization is indispensable to achieve high-speed

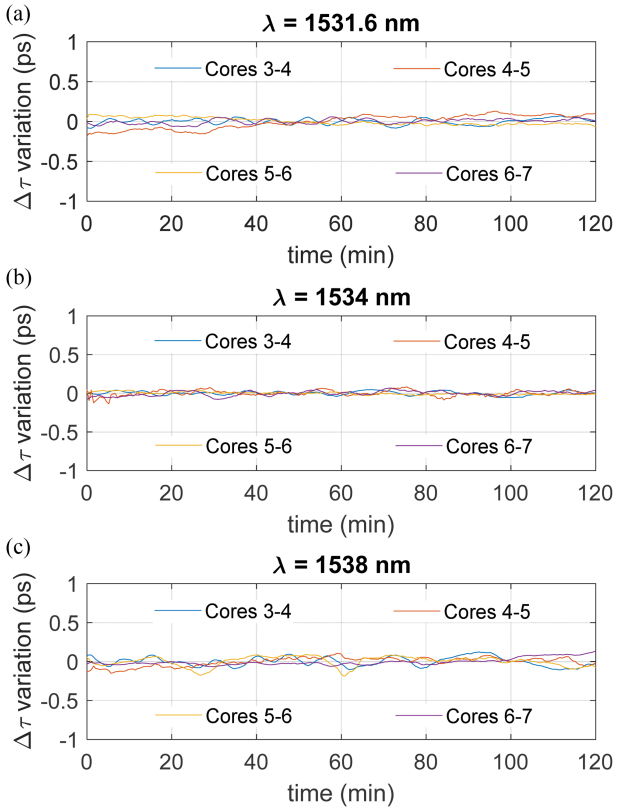

Fig. 8. Measurements of the TTDL temporal stability within a 2-hour time interval without a specific controlled environment. Variation of the differential group delay between adjacent cores as a function of time at the optical wavelength of (a) 1531.6, (b) 1534 and (c) 1538 nm.

high-performance ADCs. Another possible jitter degradation source could be caused by the temporal stability of the parallel replicas. Since the signal replicas must be adequately time synchronized at the input of the electronic ADCs, slight temporal misalignments can also introduce time uncertainty penalty and mask the low-jitter performance of the electronic ADCs involved. In this context, we have evaluated the group delay stability of the implemented TTDL. Figs. 8(a)–(c) show the measured differential group delay variation between adjacent samples within a 2-hour time interval, respectively at the optical wavelengths of $\lambda = 1531.6$, 1534 and 1538 nm. The measurements were performed in laboratory conditions but without a specific controlled environment. The maximum temperature variation was below 1 °C during the measurement time, while the humidity was kept within a 2% range. The MCF was not isolated from other environmental effects such as vibrations.

The time delay was measured via an optical interferometric based technique by calculating the fast Fourier transform of the measured interference pattern created between two adjacent samples, [23]. The maximum differential group delay variation between adjacent samples within the 2-hour measurement time interval is kept below 150 fs, while the standard deviation is below 100 fs. As we see, these values are almost on the order of the current best-case jitter characteristics of commercial electronic ADCs, so that the possible jitter penalty increase caused by the temporal stability of the MCF is almost negligible as compared with the unique performance benefits of the proposed

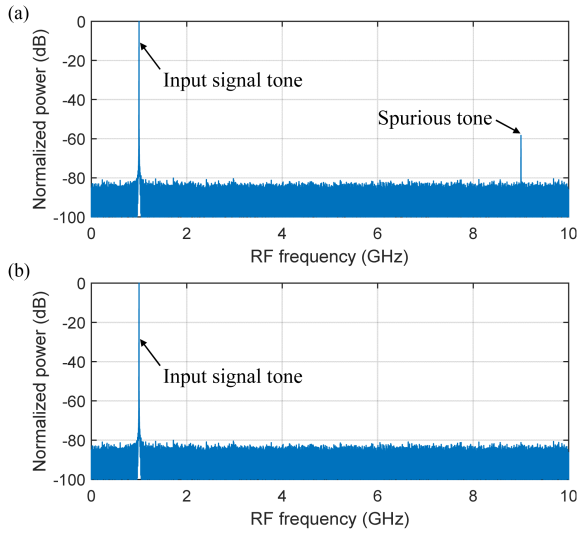

Fig. 9. Computed ADC output spectrum for a 1-GHz sinewave with both jitter and deterministic time errors: (a) without and (b) with deterministic time errors correction.

configuration, including the ADC equivalent sampling rate improvement, the continuous ADC sampling rate tunability or the remote system reconfigurability.

Lastly, deterministic time delay deviations caused by the mismatch between the actual and ideal chromatic dispersion values for each core must be adequately managed in order to improve the ADC performance. The maximum differential dispersion deviation between cores 3-7 with respect to the ideal differential dispersion of 1 ps/km/nm is 5%, what translates into a maximum $\Delta\tau$ deviation of 5%. At the optical wavelength of 1531.6 nm, this leads to a maximum differential delay deviation of 400 fs, increasing up to 2 ps at 1538 nm, much larger than the abovementioned 150-fs timing jitter. Several correction methods have been reported to digitally correct these deterministic time deviations and minimize their effects, [26], [27], [28]. As an example, we have simulated the spectrum of the ADC output with the actual time delays and jitter at the optical wavelength of 1534 nm when the input signal is a 1-GHz sinewave. Fig. 9 shows the computed ADC output spectrum of a 1-GHz sinewave (a) before correcting deterministic timing errors and (b) after its compensation. Among the many different methods that could be applied to minimize these timing errors, here we use the simplest one, which consists in applying a linear interpolation to compensate the time deviation by estimating the signal amplitude value at the proper sampling time, [27]. As we see, when the timing errors are not managed, spurious tones appear with significant amplitude and the ENOB results in 9.4, while after their correction the spurious tones are totally suppressed and the ENOB increases up to 13.3.

VI. Conclusion

We have proposed and experimentally demonstrated, for the first time to our knowledge, a new approach for photonic-assisted time-interleaved analog-to-digital conversion based on a dispersion-engineered heterogeneous MCF. The MCF is 5-km long and comprises 7 different trench-assisted cores whose

refractive index profiles were properly designed to behave as a tunable sampled TTDL. We successfully demonstrated analog-to-digital conversion with continuous sampling rate tunability with the optical wavelength from 25 up to 125 GS/s by sweeping the optical wavelength of operation from $\lambda = 1538$ down to 1531.6 nm. The measured TTDL temporal stability was within a 150-fs maximum variability range, which is in the order of the current best-case jitter performance of commercial electronic ADCs. It should be noted that one of the main advantages of using a MCF to carry the parallel channels relies on the fact that all the cavities are subject to similar environmental conditions, so that the effect of random channel misalignments are more controlled than in other parallel configurations. All in all, our approach provides unique performance benefits in terms of ADC factor multiplication sampling rate as compared to commercial electronic ADCs, continuous ADC sampling rate tunability with the optical wavelength and remote system reconfigurability.

REFERENCES

[1] G. C. Valley, "Photonic analog-to-digital converters," *Opt. Exp.*, vol. 15, no. 5, pp. 1955–1982, 2007.

[2] A. Khilo et al., "Photonic ADC: Overcoming the bottleneck of electronic jitter," *Opt. Exp.*, vol. 20, pp. 4454–4469, 2012.

[3] S. Xu et al., "Deep-learning-powered photonic analog-to-digital conversion," *Light: Sci. Appl.*, vol. 8, 2019, Art. no. 66.

[4] Y. Ma et al., "Broadband high-resolution microwave frequency measurement based on low-speed photonic analog-to-digital converters," *Opt. Exp.*, vol. 25, pp. 2355–2368, 2017.

[5] P. Ghelfi et al., "All-Optical parallelization for high sampling rate photonic ADC in fully digital radar systems," in *Proc. IEEE Opt. Fiber Commun. Conf.*, 2010, pp. 1–3.

[6] P. Ghelfi et al., "A fully photonics-based coherent radar system," *Nature*, vol. 507, pp. 341–345, 2014.

[7] K. Yoshioka et al., "A 20-ch TDC/ADC hybrid architecture LiDAR SoC for 240 x 96 pixel 200-m range imaging with smart accumulation technique and residue quantizing SAR ADC," *IEEE J. Solid-State Circuits*, vol. 53, no. 11, pp. 3026–3038, Nov. 2018.

[8] X. Jin, Z. Liu, and J. Yang, "New flash ADC scheme with maximal 13 bit variable resolution and reduced clipped noise for high-performance imaging sensor," *IEEE Sensors J.*, vol. 13, no. 1, pp. 167–171, Jan. 2013.

[9] L. Y. Nathawad, R. Urata, B. A. Wooley, and D. A. B. Miller, "A 40-GHz-Bandwidth, 4-bit, time-interleaved A/D converter using photoconductive sampling," *IEEE J. Solid-State Circuits*, vol. 38, no. 12, pp. 2021–2030, Dec. 2003.

[10] C. Xu et al., "Photonic-assisted time-interleaved ADC based on optical delay line," *J. Opt.*, vol. 18, 2016, Art. no. 015704.

[11] L. Pierno et al., "A photonic ADC for radar and EW applications based on modelocked laser," in *Proc. IEEE Int. Topical Meet. Microw. Photon.*, 2008, pp. 236–239.

[12] A. M. Fard, S. Gupta, and B. Jalali, "Photonic time-stretch digitizer and its extension to real-time spectroscopy and imaging," *Laser Photon. Rev.*, vol. 7, no. 2, pp. 207–263, 2013.

[13] L. Zhengkai et al., "Photonic sampling analog-to-digital conversion based on time and wavelength interleaved ultra-short optical pulse train generated by using monolithic integrated LNOI intensity and phase modulator," *Opt. Exp.*, vol. 30, no. 16, pp. 29611–29620, 2022.

[14] "AD9217 (2020) datasheet and product info | analog devices," Accessed: Feb. 23, 2023. [Online]. Available: https://www.analog.com/en/products/ad9217.html

[15] D. J. Richardson, J. M. Fini, and L. E. Nelson, "Space-division multiplexing in optical fibres," *Nature Photon.*, vol. 7, pp. 354–362, 2013.

[16] S. García and I. Gasulla, "Dispersion-engineered multicore fibers for distributed radiofrequency signal processing," *Opt. Exp.*, vol. 24, pp. 20641–20654, 2016.

[17] S. García, M. Ureña, and I. Gasulla, "Dispersion-diversity multicore fiber signal processing," *ACS Photon.*, vol. 9, pp. 2850–2859, 2022.

[18] M. Ureña, S. García, J. I. Herranz, and I. Gasulla, "Experimental demonstration of dispersion-diversity multicore fiber optical beamforming," *Opt. Exp.*, vol. 30, pp. 32783–32790, 2022.

[19] M. Ureña, S. García, and I. Gasulla, "Ultra-Wideband pulse generation based on dispersion-diversity multicore fiber," in *Proc. IEEE Opt. Fiber Commun. Conf.*, to be published.

[20] S. García, M. Ureña, and I. Gasulla, "Demonstration of distributed radiofrequency signal processing on heterogeneous multicore fibres," in *Proc. 45th Eur. Conf. Opt. Commun.*, 2019, pp. 1–4.

[21] S. García and I. Gasulla, "Multi-cavity optoelectronic oscillators using multicore fibers," *Opt. Exp.*, vol. 23, pp. 2403–2415, 2015.

[22] E. Nazemosadat, S. García, and I. Gasulla, "Heterogeneous multicore fiber-based microwave frequency measurement," *Opt. Exp.*, vol. 30, pp. 26886–26895, 2022.

[23] C. Dorrer, N. Belabas, J. P. Likforman, and M. Joffre, "Spectral resolution & sampling issues in Fourier-transform spectral interferometry," *J. Opt. Soc. Amer. B*, vol. 17, pp. 1795–1802, 2000.

[24] Y. Dai and J. Yao, "Nonuniformly spaced photonic microwave delay-line filters and applications," *IEEE Trans. Microw. Theory Techn.*, vol. 58, no. 11, pp. 3279–3289, Nov. 2010.

[25] B. Asuri, Y. Han, and B. Jalali, "Time-stretched ADC arrays," *IEEE Trans. Circuits Syst. II: Analog Digit. Signal Process.*, vol. 49, no. 7, pp. 521–524, Jul. 2002.

[26] C. Vogel and H. Johansson, "Time-interleaved analog-to-digital converters: Status and future directions," in *Proc. IEEE Int. Symp. Circuits Syst.*, 2006, pp. 3386–3389.

[27] H. Jin and E. K. F. Lee, "A digital-background calibration technique for minimizing timing-error effects in time-interleaved ADCs," *IEEE Trans. Circuits Syst. II: Analog Digit. Signal Process.*, vol. 47, no. 7, pp. 603–613, Jul. 2000.

[28] S. M. Jamal, D. Fu, M. P. Singh, P. J. Hurst, and S. H. Lewis, "Calibration of sample-time error in a two-channel time-interleaved analog-to-digital converter," *IEEE Trans. Circuits Syst. I: Reg. Papers*, vol. 51, no. 1, pp. 130–139, Jan. 2004.

Sergi García received the B.Sc. degree in telecommunications engineering, the M.Sc. degree in telecommunication technologies, systems and networks, and the Ph.D. degree in telecommunications from the Universitat Politècnica de València, Valencia, Spain, in 2014, 2015, and 2020, respectively, and the second B.Sc. degree in mathematics from the Universidad Nacional de Educación a Distancia, Madrid, Spain, in 2022. In 2015, he joined the Photonics Research Labs Group, iTEAM Research Institute (UPV), where he is currently a Postdoctoral Researcher. His research interests include application of space division multiplexing technologies in both multicore and few-mode fibers to microwave photonics.

Mario Ureña received the B.Sc. degree in telecommunication rechnologies and services engineering and the M.Sc. degree in telecommunications engineering from the Universitat Politècnica de València, Valencia, Spain, in 2015 and 2017, respectively. Since 2018, he has been working toward the Ph.D. degree in telecommunications engineering. In 2017, he joined the Photonics Research Labs Group, iTEAM Research Institute (UPV), where he has been working on new multicore fibers for emergent fiber-wireless communications. His research interests are optical communications, multicore fibers, and microwave photonics signal processing.

Ivana Gasulla (Senior Member, IEEE) received the M.Sc. degree in telecommunications engineering and the Ph.D. degree in telecommunications from the Universitat Politècnica de València (UPV), València, Spain, in 2005 and 2008, respectively. She is currently an Associate Professor with UPV. In 2017, she was awarded a prestigious ERC Consolidator Grant to develop new Space-Division Multiplexing technologies for emergent fiber-wireless communications through the project InnoSpace. From 2012 to 2014, she was a Fulbright Scholar with Stanford University, Stanford, CA, USA. Her research interests include application of multimode and multicore fibers to Microwave Photonics systems. The results of her work have led to more than 145 international publications, highlighting contributions to Nature Communications and Nature Photonics. She has been a Member of the TPC of the most prestigious conferences in the field, such as the Optical Fiber Communication Conference and European Conference on Optical Communications. She is a Senior Editor of IEEE JOURNAL OF SELECTED TOPICS IN QUANTUM ELECTRONICS and an Associate Editor for IEEE PHOTONICS TECHNOLOGY LETTERS.